

# IMPACT OF DIFFERENT POWERTRAIN ARCHITECTURES ON UAM VEHICLE CONCEPTS

Oliver Bertram, Florian Jäger, Viola Voth, Jan Rosenberg  
German Aerospace Center (DLR), Institute of Flight Systems, Lilienthalplatz 7, 38108  
Braunschweig, Germany

## Abstract

The research on the system architecture of Urban Air Mobility (UAM) vehicles is a vital part inside the DLR internal project HorizonUAM. One of the project goals in HorizonUAM is the development of a system concept for an air taxi. For this purpose, research is also carried out in the area of safe and certifiable onboard systems. The aim of this article is to give an overview of the previous results and findings. The system and safety challenges in the design of onboard systems with a focus on electrical powertrain systems are described. A developed preliminary design method enables full, turbo and hybrid electric drive systems to be examined in UAM vehicle design. This methodology was used in a study to investigate the influence of different powertrain architectures on the multirotor design. Here, the basic feasibility of the multirotor designs with different powertrain systems could be determined. For this purpose, the battery weight and the overall efficiency of the powertrain system were identified as design driver. There is still a need for further research into drives with fuel cell systems.

Keywords: UAM, Onboard Systems, Propulsion Systems, Preliminary Design, Multirotor, Battery, Fuel Cell, Hybrid-electric

## NOMENCLATURE

$\eta$	Component efficiency	[-]
$\kappa$	Induced power coefficient	[-]
$\mu$	Advance ratio	[-]
$\rho$	Air density	[kg/m <sup>3</sup> ]
$\sigma$	Rotor solidity	[-]
$A$	Rotor disk area	[m <sup>2</sup> ]
$C_{D0}$	Mean airfoil drag coefficient	[-]
$D_{cruise}$	Distance in cruise segment	[m]
$D_{req}$	Required total mission range	[m]
$f$	Equivalent flat plate area	[m <sup>2</sup> ]
$m$	Component mass	[kg]
$N$	Number of rotors	[-]
$P_0$	Profile power	[W]
$P_{climb}$	Climb power	[W]
$P_{cruise}$	Cruise power	[W]
$P_{in}$	Input power	[W]
$P_{out}$	Output power	[W]
$P_{hover}$	Hover power	[W]
$P_p$	Parasitic power	[W]
$P_{vertical}$	Total climb or descent power	[W]
$SE$	Specific energy	[Wh/kg]
$SP$	Specific power	[W/kg]
$T/A$	Disc loading	[N/m <sup>2</sup> ]
$V_{climb}$	Climb rate	[m/s]
$V_{cruise}$	Cruise speed	[m/s]
$V_{hover}$	Hover speed	[m/s]
$V_{tip}$	Rotor blade tip speed	[m/s]
$W$	Aircraft weight	[N]

## 1. INTRODUCTION

As part of the HorizonUAM project, research is being carried out at the German Aerospace Center (DLR) in the field of Urban Air Mobility (UAM), i.e. the expansion of urban transport systems into the airspace [1]. Efficiency, safety, practicability, sustainability and affordability are just a few features that describe the vision of future urban mobility. The HorizonUAM project aims to provide initial answers to this vision. The project focus is, among other things, on the

vehicle, infrastructure and operation as well as acceptance.

In UAM concepts, autonomous flying taxis are seen as an important element. A large number of different prototypical air taxi concepts already exist today, which differ from conventional aircraft in terms of their vertical take-off and landing capabilities (VTOL). The distinction to conventional rotary wing aircraft, on the other hand, is based on the use of distributed, electric drives, in particular if more than two lift and / or thrust units are used to generate lift during vertical take-off or landing.

One of the project goals in HorizonUAM is the development of a system concept for an air taxi. For this purpose, the Safety-Critical Systems and Systems Engineering department at the DLR Institute of Flight Systems conducts research in the field of safe and certifiable onboard systems. The research is carried out in three main areas of work.

The first area of work includes a literature research on the current state of the art of onboard systems. Relevant technologies, subsystems and commercially available equipment are to be identified, analyzed and summarized. In addition, suitable conceptual design methods should be determined and research questions identified.

A suitable process and tool chain are required for a model-based design approach of the onboard systems. For this purpose, the necessary requirements are defined and the sizing process implemented. For the conceptual design, suitable design and sizing methods are developed and implemented in the tools.

System architectures are to be defined, dimensioned and investigated in a final step. The aim of these investigations is to identify and analyze the influence of the systems design on the overall configuration. This is intended to determine the basic understanding of the challenges in the onboard systems design and to ensure the feasibility of an onboard system concept for the planned air taxi system concept.

The aim of this article is to give an overview of the previous results and findings of the research described above. For

this purpose, chapter 2 describes the challenges in the design of the onboard systems identified by the literature research. There is a special focus on electric drive systems. System and safety-related challenges and essential design and approval aspects are presented. Chapter 3 describes a developed preliminary design method that enables full-, turbo- and hybrid-electric powertrain systems to be investigated. In chapter 4, this methodology is applied in the context of a first design study that has been carried out. The study results are presented and discussed. These findings are to flow into the overarching system concept of the air taxi. Chapter 5 gives a summary and an outlook on the further planned activities with regard to the onboard systems in the context of the HorizonUAM project.

## 2. ONBOARD SYSTEM DESIGN CHALLENGES

At the beginning, a literature research on the current state of the art of onboard systems was carried out [2]. The aim of the research was to identify relevant technologies, subsystems and commercially available equipment as well as suitable conceptual design methods.

A large number of different UAM vehicle concepts already exist today [3]. Most of the concepts are prototypical developments that still require a lot of research. Only a few concepts are on the way to approval, such as the VoloCity. Based on studies carried out by NASA, various research areas for UAM vehicles were identified [4]. These areas are shown in FIGURE 1. Further research fields include autonomy, approval processes, communication and navigation as well as technology integration.

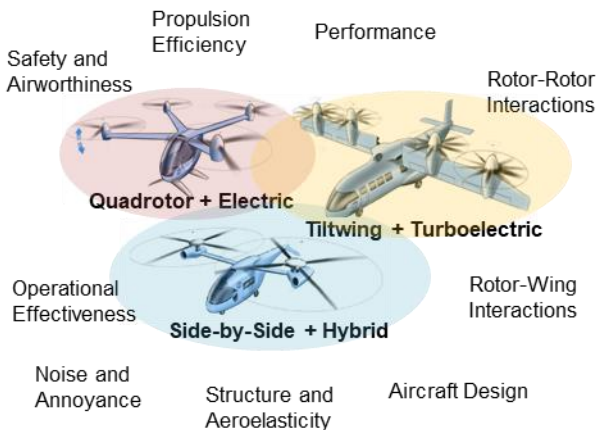


FIGURE 1. Research fields for UAM vehicle concepts [4]

Basically, the design of an aircraft is highly complex and multidisciplinary, with a wide variety of interactions and influences between the different design disciplines. The description of the various interactions would exceed the scope of this article. Therefore, only the aspects related to the electric powertrain system are considered in more detail below. The overall goal of this paper is to assess the suitability and potential drive trains in UAM vehicles.

### 2.1. Power Requirements

A distinction can be made between air taxis, for instance, in cruise configurations with rotating wings (e.g. multirotor, conventional and coaxial helicopters) and cruise configurations with fixed wings (e.g. lift and cruise, tilt duct, tilt wing). From a flight performance-based perspective, these different configurations are typically characterized by

their hovering and cruising efficiency. Values of the design variables mentioned above can be found in the literature and can provide an initial estimate for the design space of potential aircraft architectures [5].

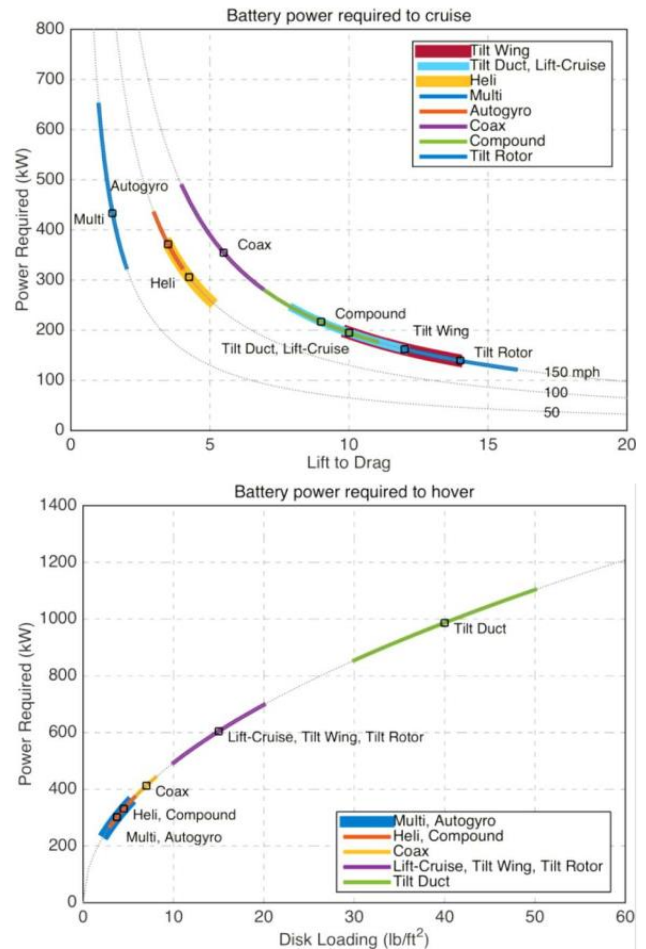


FIGURE 2. Battery electric power requirements in cruise and hover for different vehicle configurations [5]

Due to the flight performance, different aircraft configurations also have different battery power requirements. This fact is shown in FIGURE 2 for an exemplary MTOM of 2268 kg at ISA MSL (mean sea level) for cruise flight and hover. For other flight phases, environmental conditions and mission requirements such as cruise speed, payload, reserves, etc., these power requirements differ and thus the battery size and dimensions change with a strong impact on the overall size and weight of the aircraft. FIGURE 2 shows also that the battery power requirements strongly depend on the aircraft configuration and its related lift-to-drag and disc loading characteristics.

### 2.2. System Technology Aspects

Today, electric powertrain and battery technologies are the enablers for the implementation of electric air taxi concepts (eVTOL). Electric powertrains are simpler than gas turbines and mechanical drive trains and have lower maintenance costs, which leads to lower vehicle costs. In addition, electric drives are emission-free, low-noise and “green” if sustainable energy is used. From a safety and reliability perspective, decentralized, distributed electrical drive concepts play a major role. In addition, battery costs are falling continuously due to the high demand and production in the automotive industry.

The battery technology available today, however, ends in a relatively high component weight with reduced payload capacity and enables only short flight times or ranges in eVTOL applications compared to an aircraft with a conventional propulsion system. This has a major impact on the vehicle design as well as on operational aspects of the individual eVTOL, the entire eVTOL fleet or, in other words, on the system of systems.

However, with increasing battery technological parameters such as specific power or energy density, for example, the payload ratio and the ranges increase accordingly. In order to meet these challenges in today's battery technology, alternatively turbo- or hybrid-electric powertrain concepts can be used as bridge technology. Exemplary system architectures can be found, for instance, in [6] and [7].

In addition, fuel cell systems can also be used as an electrical energy source. However, these systems bring new requirements, e.g. on the cooling or tank system. However, the use of fuel cell systems enables a continuous electrical energy output for higher endurance of the vehicle, a pollutant-free, environmentally friendly reaction process and a noiseless functionality [8]. Short-term peak performances (e.g. during take-off or landing) can be provided in conjunction with a battery system. So far, no approved air taxi that is powered by a fuel cell system has been developed anywhere in the world. Challenges and research needs lie in the crash safety of the hydrogen-carrying components, the liquid or gaseous storage of hydrogen, the limited service life and the higher system weight.

In the field of electric powertrain architectures, research is taking place to increase the specific power and overall efficiency in order to reduce the weight of the drive system the amount of heat to be dissipated, and to decrease the required power level.

### 2.3. Safety-Critical Design Aspects

Electric propulsion systems face aircraft designers and safety engineers with new and unknown challenges. The new danger in eVTOLs are lithium batteries, which can fail in seemingly more complex modes. The main danger here is the thermal runaway, if rapid, self-sustaining increases in temperature and pressure occur in battery cells and can lead to an external fire. Reasons for thermal runaway can be, for example, deep discharge, overcharging and internal short circuits. Toxic gases can also be released and crash safety must be guaranteed. [6]

In addition, electrical high-voltage systems represent another new type of danger in flight when energy is released through short circuits and arcs. This at least leads to a deterioration in the performance of the powertrain system and could also lead to a fire. At the same time, however, high-voltage systems also pose a risk for maintenance and ground handling personnel.[6]

However, the electric powertrain systems also offer new potential for increasing safety. For example, aircraft with distributed, electric propulsion can be more tolerant of bird strikes and engine losses than previous propulsion configurations. In the design, the individual components can be designed redundantly and networked with one another in such a way that the failure of individual

components does not lead to a safety-critical situation. There are also more options of redistributing the power to other drives in the event of a component failure than with mechanical drive trains. This enables simpler, less complicated and more effective system architectures. [6]

In summary, electric powertrain systems have the potential to improve system safety in the event of failure conditions and eliminate hazards associated with jet fuel. At the same time, however, new threats are being introduced, such as the thermal runaway of battery packs. Methods to demonstrate the safety of electrical systems, demonstrator service experience, and best design practices will be critical to reducing risk in this area. [6]

### 2.4. Certification Aspects

In order to be allowed to operate eVTOLs in European airspace, this type of aircraft also requires a type certification by EASA. Due to the increasing number of inquiries on this topic and the lack of suitable certification regulations, EASA has published a complete set of technical specifications in the form of a "Special Condition Vertical Take-Off and Landing Aircraft" (SC-VTOL) [9]. Since the VTOL aircraft currently under development have the properties of conventional aircraft and helicopters, but at the same time there are also serious differences such as the distributed drive units, individual aspects from the certification regulations CS-23 for smaller aircraft and CS-27 for small helicopters are included in the special condition and supplemented with new regulations specially adapted to the unique characteristics of VTOL aircraft. In addition, the first edition of the "Proposed Means of Compliance with the Special Condition VTOL" was released for public consultation and comment [10]. A first set of Accepted Means of Compliance (AMCs) can be found in this document. This enables individual paragraphs of the special condition to be verified. However, the document will only become binding after the public consultation phase and the transition to Accepted Means of Compliance. By using a special condition, EASA was able to react quickly to the growing number of certification questions relating to VTOL-capable aircraft and not have to initiate the much longer process of creating a certification specification. However, this is to be done later on and on the basis of the knowledge gained through the application of the SC-VTOL. Until the publication of a final "CS-VTOL", the special condition serves as an interim solution.

The SC-VTOL defines the general requirements for the aircraft, which are not restricted to specific systems and components:

- Passenger, VTOL-capable aircraft of the "small" category that are heavier than air
- Maximum capacity of 9 or fewer passengers
- Maximum certified take-off weight of 3,175 kg or less
- Aircraft must have at least two lift / drive units that are used to generate lift during the vertical take-off or landing phase and to control the aircraft.
- Restriction only for aircraft that are not pressurized and whose maximum calibrated speed in normal operation does not exceed 250 knots or Mach 0.6

Certification takes place either in the "basic" or "enhanced" category. A grouping in the category "enhanced" has to take place if an operation over metropolitan areas is planned or if the aircraft is to be used for the commercial transport of people, which is usually the case with air taxis. For these aircraft, it must be proven that they are still able

to make a safe onward flight and a safe landing (CSFL, "Continued Safe Flight and Landing") on one of them provided vertiport without the requirement of extraordinary pilot skills, for the case of a single failure not classified as catastrophic or a catastrophic combination of failures. With regard to the configuration in the project, these requirements are more than sufficient.

A description and analysis of the individual requirements of the SC-VTOL e.g. on the electric powertrain system should not be further carried out here. In general, however, every system or its component must be installed in accordance with its applicable limitations. When developing the systems, it should be noted that

- every catastrophic failure is "extremely improbable" and cannot occur as a result of a single failure,
- every hazardous failure case is "extremely remote" and
- every serious failure is "remote".

Systems whose failure condition could lead to a catastrophic or hazardous event must be able to be monitored by means of suitable monitoring during operation. The operation of other systems that do not have to meet these requirements must also not pose a risk to the aircraft or the occupants in the entire operating area. According to the proposed AMCs, all failures that prevent the aircraft from safely continuing its flight and landing are to be classified as catastrophic in the context of the safety analysis. The failure rates to be verified and the "Function Development Assurance Level" (FDAL) to be used for the individual failure categories can be found in TAB 1.

TAB 1. Failure rates and FDAL of the individual failure categories [9]

Category	Max. PAX	Classification			
		MIN	MAJ	HAZ	CAT
Enhanced	-	$\leq 10^{-3}$	$\leq 10^{-5}$	$\leq 10^{-7}$	$\leq 10^{-9}$
		FDAL D	FDAL C	FDAL B	FDAL A
Basic	7-9 PAX	$\leq 10^{-3}$	$\leq 10^{-5}$	$\leq 10^{-7}$	$\leq 10^{-9}$
		FDAL D	FDAL C	FDAL B	FDAL A
	2-6 PAX	$\leq 10^{-3}$	$\leq 10^{-5}$	$\leq 10^{-7}$	$\leq 10^{-8}$
		FDAL D	FDAL C	FDAL C	FDAL B
	0-1 PAX	$\leq 10^{-3}$	$\leq 10^{-5}$	$\leq 10^{-6}$	$\leq 10^{-7}$
		FDAL D	FDAL C	FDAL C	FDAL C

MIN: Minor; MAJ: Major; HAZ: Hazardous; CAT: Catastrophic

### 3. MODEL-BASED DESIGN METHODOLOGY

In the last chapter, the challenges in the design of electrical powertrain as part of the onboard systems were presented. The entire onboard system consists of various subsystems such as flight control, avionics, etc. with a large number of components. A large number of system-related questions arise from the literature research, particularly for electrical powertrains. These range from a suitable definition of the system architecture and the technology level, the safety-critical design, parameter, sensitivity and feasibility studies to the validation and verification of the requirements.

A model-based design methodology is presented in this chapter. This methodology should make it possible to carry out conceptual studies and to examine the influence of

different electric and hybrid-electric powertrain architectures on the eVTOL design in an early design phase. Safety and reliability play a very important role for design and approval (see sections 2.3 and 2.4) but have not yet been considered in the methodology. Rather, the purpose is to preselect feasible concepts and transfer them to a subsequent, detailed design step with safety and reliability analyzes.

#### 3.1. Methodology Definition

A model-based approach was chosen as part of the project. This approach should make it possible to answer relevant questions, to allow investigations of influences and interactions in the design of the eVTOL and the overall system of systems and to contribute to the design of the air taxi system concept.

A conceptual design method was developed for the model-based approach, which is shown in FIGURE 3. The methodology consists of the three main steps

- Definition of inputs,
- Sizing loop and
- Design analysis.

These steps are explained in more detail in the following sections.

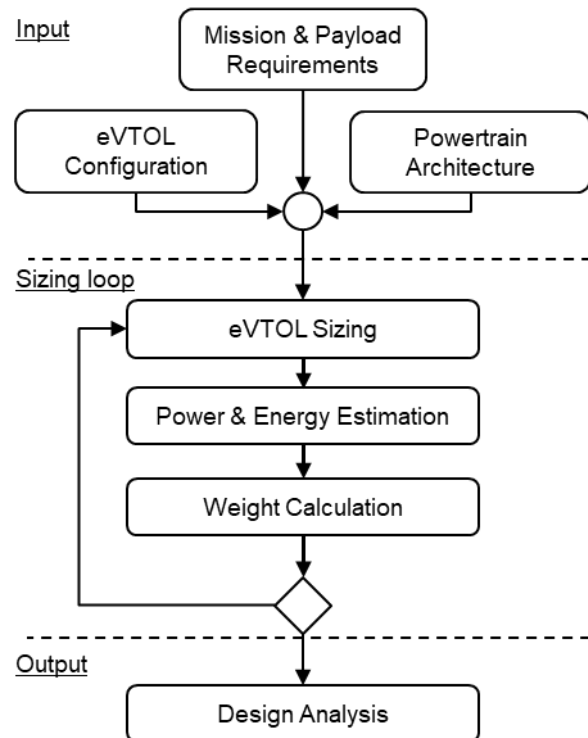


FIGURE 3. Conceptual design methodology

##### 3.1.1. Input Definition

Three input categories are required for the methodology. The first category includes the mission and payload requirements. During the HorizonUAM project, for example, various use cases such as intra-city, airport shuttles, etc. with associated TLARs were defined and technology assumptions were made for the years 2025 and 2050. The profile for the design reference mission is shown in FIGURE 4 along with the specific TLARs for this study.

Second, the eVTOL configuration must be defined with size-relevant parameters such as the initial, maximum total take-off mass (MTOM), disc loading and number of rotors.

Other input parameters are listed in TAB 2. In principle, there are no restrictions in the choice of configuration and parameters. In HorizonUAM it was agreed to investigate a multirotor configuration for the air taxi system concept. Therefore, the focus is on this configuration.

The third category defines the powertrain architecture. In addition to full-electric systems (battery or fuel cell), turbo- or hybrid-electric system architectures can also be used as bridging technology. Each individual powertrain architecture consists of a set of components such as electric motors, generators, power electronics, gas turbines, gears, rotors, etc., which are connected to one another. The definition of the architecture should make it possible to answer different design and research questions. The inputs described are finally put into the sizing loop, which is described in the next section 3.1.2.

### 3.1.2. Sizing Loop

The sizing loop shown in FIGURE 3 comprises the eVTOL sizing, the power and energy estimation and the weight calculation of the structural and system components.

Based on the input data, an initial eVTOL sizing is carried out with regard to the mission requirements and an initial MTOM. For this purpose, a performance model of the multirotor was developed based on the momentum theory, respectively actuator disc. This model is described in more detail in section 3.2.1 and is used to calculate the flight performance in each individual flight phase of the mission.

The performance and energy estimations for the systems are carried out on this basis. For this purpose, a calculation network is set up and solved for each defined powertrain architecture. The powertrain model is described in section 3.2.2. As a result, the power requirement for each individual powertrain component as well as the overall energy requirement of the mission is determined.

On the basis of the performance and energy parameters the weights of the components and energy sources (battery, kerosene, hydrogen) of the powertrain system are then determined. In addition, the weight of structural components and other systems such as flight control, environmental control system, avionics is estimated using simplified models and assumptions (see section 3.2.3). The calculated weights of all components are used to determine a new total weight for the eVTOL.

Finally, the convergence is checked. As long as the convergence criterion is not met, the MTOM is updated with these component weights and the next iteration begins. Also, other configuration parameters like rotor disk area, rotor radius are updated with each iteration. If the criterion is met, the results of each converged solution are provided as output for the subsequent design analysis.

### 3.1.3. Design Analysis

In the design analysis, the results of the sizing loop are analyzed with regard to the design and research questions. The output includes the component and group weights as well as the weight proportions for the eVTOL with different powertrain architectures. In addition, powertrain efficiency is addressed and analyzed (see section 4.2).

## 3.2. Sizing and Performance Models

The following section describes the different sizing and performance models that are used in the sizing loop.

### 3.2.1. Flight Performance Model

To calculate the flight performance of the multirotor, a performance model based on the momentum theory was developed from the literature [11]. The momentum theory is the simplest theory for estimating the performance. The rotor is abstracted as an actuator disc, whereby the number and design of the rotor blades, the rotor hub, the fuselage etc. are not considered. The momentum theory means a significant reduction in the highly complex aerodynamic processes on the rotor. The flow itself is assumed to be one-dimensional, quasi-stationary, incompressible and frictionless. In Ground Effects (IGE), Side-by-side effect [12] or the Angle of Attack (AoA) were also neglected. Finally, the basic equations for the conservation of mass, momentum and energy were used to determine the essential relationships as a basis for determining the required performance. Based on these relationships, the required flight performance in the various flight phases was determined.

#### Hover Performance

An important characteristic is the hover performance  $P_{\text{hover}}$ , which is made up of the profile performance  $P_0$ , i.e. the zero drag of the rotor blade profiles, and the real, induced performance  $P_{i,\text{hover}}$ .

$$(1) P_{\text{hover}} = P_0 + P_{i,\text{hover}}$$

The induced hover performance can be estimated with the air density  $\rho$  and the induced power coefficient  $\kappa$ , which are assumed as constant. The rotor disk area  $A$  and the weight  $W$  are variable parameters related to the current iteration of the multirotor configuration.

$$(2) P_{i,\text{hover}} = \kappa \cdot W \cdot \sqrt{\frac{W}{2 \cdot \rho \cdot A}} \cdot \frac{1}{V_{i,\text{hover}}}$$

The profile power can be estimated with the blade tip speed  $v_{\text{tip}}$ , the solidity  $\sigma$ , the mean airfoil drag coefficient  $C_{D0}$  and the tip speed ratio  $\mu$ . In case of hover, the cruise speed is zero and thus the tip speed ratio  $\mu$  is omitted.

$$(3) P_0 = \rho \cdot A \cdot v_{\text{tip}}^3 \cdot \frac{\sigma}{8} \cdot C_{D0} \cdot (1 + 4.5 \cdot \mu^2)$$

$$(4) \mu = \frac{v_{\text{cruise}} \cdot \cos \alpha}{\Omega \cdot R} \approx \frac{v_{\text{cruise}}}{v_{\text{tip}}}$$

#### Performance in Vertical Climb and Vertical Descent

The total power in vertical climb (or respectively descent) can be estimated with the profile power  $P_0$ , the climb power  $P_{\text{climb}}$  and the induced power for axial climb  $P_{i,\text{climb}}$ .

$$(5) P_{\text{climb,total}} = P_0 + P_{i,\text{climb}} + P_{\text{climb}}$$

The climb power is calculated with the aircraft weight  $W$

$$(6) P_{\text{climb}} = W \cdot v_{\text{climb}}$$

According to [11] and [12], the induced power for axial climb  $P_{i,\text{climb}}$  can be computed in relation to the induced hover power. This equation can be used for small climb or very small descent rates, which is the case in this paper. For

higher vertical speeds, especially in descent, this formulation may lose validity.

$$(7) P_{i,climb} = P_{i,hover} \cdot \left[ \frac{v_{climb}}{2 \cdot v_{i,hover}} + \sqrt{\left( \frac{v_{climb}}{2 \cdot v_{i,hover}} \right)^2 + 1} \right]$$

### Cruise Performance

Normally, the angle of attack (AoA) of the blade tip path plane tilts the thrust vector forward and allows the multirotor to accelerate and cruise. Assuming that this angle is neglected ( $\alpha=0^\circ$ ) and thrust equals weight ( $T=W$ ), rough analytical solutions for the required cruise performance can be used. According to [12], the cruise performance can be determined using the profile power  $P_0$ , the induced power  $P_{i,cruise}$  and the parasitic power  $P_{p,cruise}$ . In case of cruise climb (or descent), the climb power is additionally required:

$$(8) P_{cruise} = P_0 + P_{i,cruise} + P_{p,cruise} + P_{climb}$$

The power induced during cruise can be determined via the cruise speed  $v_{cruise}$ , the induced speed in hover  $v_{i,hover}$  as well as the weight  $W$  and the induced power coefficient  $k$ .

$$(9) P_{i,cruise} = k \cdot W \cdot \sqrt{-\frac{v_{cruise}^2}{2} + \sqrt{\frac{v_{cruise}^4}{4} + v_{i,hover}^4}}$$

Power losses resulting from friction and flow separations on the airframe, the rotor hub, landing gear, antennas etc. are considered and treated as parasitic power  $P_p$ . For this purpose, an equivalent flat plate area  $f$  must be assumed or otherwise determined [12].

$$(10) P_{p,cruise} = 0.5 \cdot \rho \cdot f \cdot v_{cruise}^3$$

### Cruise Speeds for Best Endurance and Best Range

In addition to the performance parameters listed above, the cruise speeds for best range  $v_{br}$  and best endurance  $v_{be}$  can be determined analytically according to [11].

$$(11) v_{cruise,br} = \sqrt{\frac{W}{2 \cdot \rho \cdot A}} \cdot \left( \frac{4 \cdot k}{f/A} \right)^{0.25}$$

$$(12) v_{cruise,be} = \sqrt{\frac{W}{2 \cdot \rho \cdot A}} \cdot \left( \frac{4 \cdot k}{3 \cdot f/A} \right)^{0.25}$$

For this, the rotor disk area  $A$ , the equivalent flat plate area  $f$ , the induced velocity in hover and the empirically determined induced power coefficient  $k$  are required. In the context of this work, the value of  $k$  is assumed to be 1.15 in a first approximation. The determined cruise speeds are used in different flight phases. An assignment can be found in the definition of the mission segments for the study carried out (see TAB 3).

### 3.2.2. Powertrain Model

In the following, an analytical, stationary model for the design of electrical powertrain architectures is presented for the estimation of the power and energy quantities. This model is based on the work of de Vries [7] and is used to calculate the power of each individual powertrain element for a given flight performance requirement. This performance requirement is calculated using the eVTOL performance model.

Based on the specified performance requirements, the model should also offer the option of calculating various powertrain architectures. De Vries suggested different (hybrid) electrical architectures for his model [7]. His investigations showed that the Serial / Parallel Partial Hybrid (SPPH) architecture can be used as a general model to configure and calculate other hybrid and fully electric architectures using two power control parameters, namely the supplied power ratio  $\Phi$  and the shaft power ratio  $\phi$ . With the help of these power control parameters, a subsequent analysis and optimization of the power settings during the mission can be also made possible [7]. However, this is not part of this work.

For this work, the supplied power ratio  $\Phi$  is relevant. This ratio represents the amount of energy taken from the electrical energy source (e.g. batteries) in relation to the total amount of energy that is taken from all energy sources (e.g. kerosene, batteries, hydrogen) for a specific point of the mission. As part of the study carried out (see chapter 4), the proportion of the electrical power consumed is varied for the hybrid-electric powertrain architectures ( $\Phi = [0.2, 0.5, 0.8]$ ).

The powertrain model consists of a total of ten unknown power quantities. Hence, ten equations are needed to solve the system. These quantities and equations are not shown here and reference is made to [7]. Three of the ten equations are utilizing the power control parameters  $\Phi$  and  $\phi$  as well as the flight performance. The other equations give the power balance for each of the seven powertrain components. In order to create a balance between the incoming and outgoing power quantities of a component, the corresponding component efficiency  $\eta$  is specified, see equation (13).

TAB 4 gives an overview of the component efficiencies used in this study. The linear system of equations created is finally solved by entering the flight performance requirement for each flight phase. As a result, the required power of the individual components is calculated for each phase.

$$(13) P_{out} = \eta \cdot \sum P_{in}$$

On the basis of these calculated power parameters, the component weights for the motors, power electronics, etc. are finally calculated using the specific power values  $SP$  and sized to the maximum power. The values used for each individual component are also listed in TAB 4.

$$(14) m_{component} = \frac{P_{component, max}}{SP_{comp}}$$

The model of de Vries does not consider the design of fuel cell systems as an electrical energy source. To make this possible, a corresponding model with efficiency and specific power was added. There are two possible architectures with a fuel cell system (see FIGURE 5). Either the fuel cell system can completely replace the battery if it is assumed that the correspondingly high power and currents can be provided by the fuel cell. Alternatively, the fuel cell can be operated in conjunction with the battery, i.e. as an energy source used in parallel. For this it is assumed that the fuel cell provides a constant, maximum power in cruise and is designed for this, while the battery covers the additional peak power, e.g. in vertical climb or hover. The weight of the fuel cell is also calculated using the specific power. Furthermore, the fuel cell cooling system is calculated with



50% of the mass of the fuel cell.

In contrast to the components mentioned above, the mass calculation of the fuel  $m_{Fuel}$  or the hydrogen  $m_{Hydrogen}$  is not based on the power, but on the energy requirement. In addition to the required power, the duration of the respective output is determined via the mission profile. The specific energy for kerosene  $SE_{Fuel}$  or for hydrogen  $SE_{Hydrogen}$  is used for the calculation (see TAB 4).

$$(15) m_{fuel} = \frac{E_{fuel}}{SE_{fuel}}$$

$$(16) m_{hydrogen} = \frac{E_{hydrogen}}{SE_{hydrogen}}$$

The influence of the reduction of the fuel or hydrogen mass over the mission is neglected in the model, since these masses are rather small compared to other component masses in the multirotor design. This means that the influence of the decrease on the aircraft mass can be neglected in a first approximation.

The calculation of the battery mass  $m_{Bat}$  is based on both the power and the energy requirement and thus differs from the other components of the electric powertrain. The battery mass is determined from the maximum value of both requirements. For this, the battery efficiency  $\eta_{Bat}$ , the minimum and maximum depth of discharge and the C-rate are taken into account. The C-rate is the current in which a battery is charged and discharged at, related to the battery capacity. Other parameters such as the state of charge (SoC) or the system voltage have been neglected in this design model for the sake of simplicity.

$$(17) m_{Bat} = \max\left(\frac{P_{bat, max}}{SP_{bat}}, \frac{E_{bat}}{SE_{bat}}\right)$$

### 3.2.3. Model for Other Systems

While various powertrain architectures can be considered and calculated, the other systems such as flight control, avionics, instrumentation, furnishings and environmental control system are combined in a general model that was taken from [13].

$$(18) m_{other,sys} = 0.0239 \cdot m_{MTOM} + 195.71$$

This model requires the maximum take-off mass of the aircraft (MTOM) as an input variable in order to determine the system weight using a linear approach. It should be noted that the model works with the unit [lb] and therefore the input and output values must be converted into the unit [kg]. In the future, the modeling of these onboard systems is to be improved, for example by considering the systems as a mission-dependent, electrical load when designing the powertrain. Further models for determining weight can be found in [14].

### 3.2.4. Structure Mass Estimation Model

In addition to the systems, the structural masses must also be estimated for the dimensioning of the multirotor. Equations for mass estimation for wings, empennage, rotor and hubs, as well as landing gear and fuselage can be found in [14]. However, due to the configuration, the masses for the wings and empennage are omitted with the multirotor. In addition to specifying various parameters such as number of rotors, number of wheels, etc., the equations

are primarily based on the input variable aircraft mass or thrust, so that the structural masses as well as the system masses change with each iteration.

## 4. DESIGN STUDY

One goal in the HorizonUAM project is to develop a system concept for an air taxi. As part of different studies, the onboard systems are to be examined in more detail and the findings are to be incorporated as a contribution to the concept. The aim of this first study is to investigate the impact of different powertrain architectures on the multirotor design. First important findings should be found and, if possible, suitable and feasible architectures should be identified, which should be examined more closely in the future. The design methodology developed and described in section 3 was used for this purpose. This section describes the procedure and the findings so far.

### 4.1. Study Definition

#### 4.1.1. TLARs and Mission

An intra-city use case was defined for the study. The transport task is to carry out on-demand and non-stop flights within the core area and the densely populated areas of a city. Short transport ranges of up to 50 km ( $=D_{req}$ ) between vertiports and vertistops are to be covered at a speed of up to 100 km/h. The multirotor configuration with 4 seats including a pilot (or autonomous without a pilot) is particularly suitable for this use case. The payload is 90 kg per person, i.e. a total of 360 kg. Further parameters for the configuration can be found in TAB 2

TAB 2. Multirotor configuration parameters

Parameter	T/A	Value
Disc loading		140 N/m <sup>2</sup>
Number of rotors N	N	4
Rotor blade tip speed	$V_{tip}$	153 m/s (M=0.45)
Equivalen flat plate area	f	3 m <sup>2</sup>
Solidity	$\sigma$	0.06
Profile zero drag coefficient	$C_{D0}$	0.01
Induced power coefficient	$\kappa$	1.15

The mission profile used in the study is presented in FIGURE 4. For each segment, the allocated flight performance is also shown. For example, the performance in the start and shutdown segment is simply calculated with 10% of the cruise performance. Further definitions of the mission segments are given in TAB 3. To simplify the flight performance calculation, the air density at mean sea level is assumed ( $\rho = 1,225 \text{ kg/m}^3$ ).

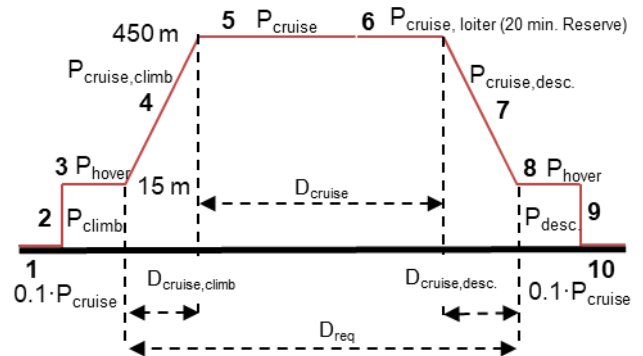


FIGURE 4. Sizing mission profile

TAB 3. Mission segment definitions

Segment	Cruise Speed [m/s]	Climb Rate [m/s]	Distance [km]	Time [min]
1 Start up				0.3
2 Vertical Climb		0.5		0.5
3 Transition	0 to $V_{cruise,be}$			1
4 Cruise Climb	$V_{cruise,be}$	4	$D_{cruise,climb}$	$t_{cr,climb}$
5 Cruise	$V_{cruise,br}$		$D_{req}$ - $D_{cruise,climb}$ - $D_{cruise,desc}$	$t_{cr}$
6 Loiter	$V_{cruise,be}$		-	20
7 Cruise Descent	$V_{cruise,be}$	- 4	$D_{cruise,desc}$	$t_{cr,desc.}$
8 Transition	$V_{cruise,be}$ to 0			1
9 Vertical Descent		- 0.5		0.5
10 Shut down				0.3

#### 4.1.2. Powertrain Architecture Definition

For the powertrain, both full and hybrid-electric architectures and their impact on the design are to be examined. FIGURE 5 provides an overview of the simplified models of the defined architectures.

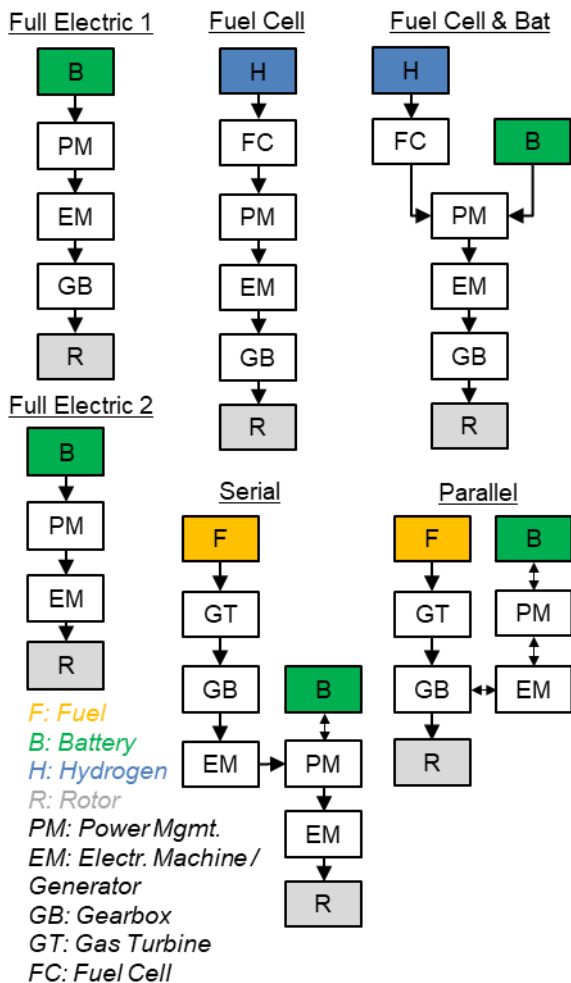


FIGURE 5. Simplified powertrain models

In addition to two full electric architectures with a battery as an energy source two hybrid-electric powertrains (serial, parallel) are being investigated. The supplied power ratio is varied for both hybrid electrical architectures ( $\Phi = [0.2, 0.5, 0.8]$ ), so that a total of six variants can be examined. The higher the value for the supplied power ratio, the closer the two variants come to the two full electric architectures. For the last two architectures, hydrogen-based fuel cell systems are being investigated as an electrical energy source. In case of "Fuel Cell" no battery is used, while in case of "Fuel Cell & Bat", a battery is operated in parallel with the fuel cell system. The system was modeled in such a way that the fuel cell is designed for the cruise power and can also provide this power continuously. The battery, on the other hand, provides the peak power.

In order to examine the general feasibility of the concepts, the technology level available today is assumed and considered in the design method. Any technological improvement and its impact on the design are not to be examined in this study. The technology parameters used in the study for the various components are listed in TAB 4.

TAB 4. Component technology parameters

Powertrain Component	Specific Power	Specific Energy	Efficiency
Gas turbine	8.2 kW/kg	-	0.50
Gear box	5 kW/kg	-	0.98
Rotors	3 kW/kg	-	-0.87*
Generator	4 kW/kg	-	0.95
Power Mgmt.	5 kW/kg	-	0.98
Electr. Motors	4 kW/kg	-	0.95
Fuel Cell Stack**	1.6 kW/kg	-	0.5
Kerosene	-	11.8 kWh/kg	-
Hydrogen	-	33.3 kWh/kg	-
Battery	625 W/kg	250 Wh/kg	0.96
	C-Rate: 2.5; Useable energy factor: 0.8; Packaging factor: 0.35		

\*considered in the flight performance model  
\*\* Fuel cell system mass is 3 times of fuel cell stack mass

#### 4.1.3. Evaluation Criteria (Metrics)

After the definition of the mission and the architectures to be examined, evaluation criteria were also set up with which the different concepts are to be compared and their impact on the design determined. These criteria are:

- Maximum take-off weight (MTOW) [kg],
- Weight breakdown in groups [kg],
- Weight fractions [kg/MTOW]
- Required power [kW/time] and energy (kWh)
- Energy efficiency [Energy/Pax.km]
- Charging power [kW]

#### 4.2. Study Results Analysis

##### 4.2.1. Aircraft Masses

FIGURE 6 shows the maximum take-off mass for the examined hybrid- and full electric powertrain systems. Basically, it can be stated that a solution could be found for every configuration on the basis of the defined study (the convergence criterion was met). All solutions are also below the maximum allowable take-off mass of 3,125kg (see



section 2.4). The lowest aircraft mass can be found with the two hybrid-electric architectures and a low power ratio  $\Phi$ . The higher the supplied power ratio, the higher the aircraft weight. The fuel cell system has the highest mass.

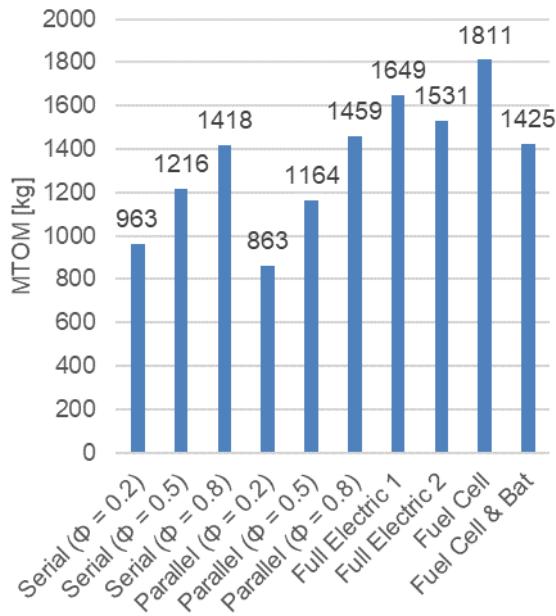


FIGURE 6. Maximum take-off masses

FIGURE 7 shows the empty mass and payload fractions for the various systems. Although the absolute value of the payload is constant at 360 kg, the relative share decreases as the power ratio increases. The lowest proportion of the payload can also be observed for the fuel cell powertrain system.

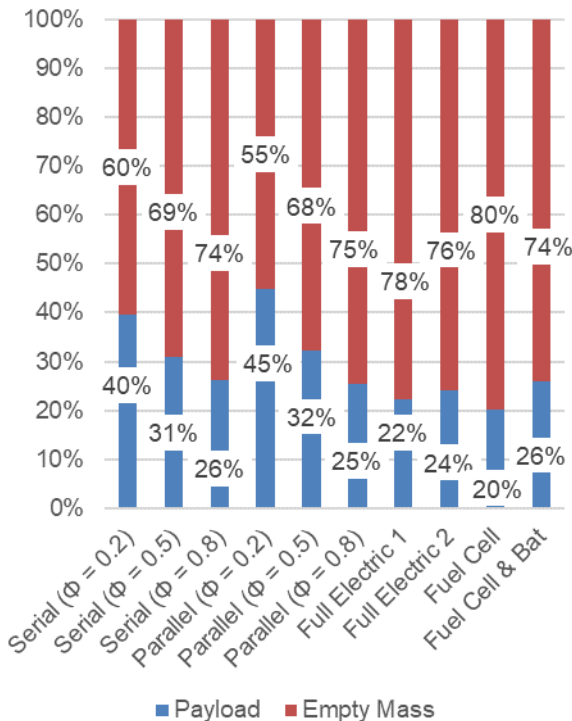


FIGURE 7. Empty mass and payload fraction

In order to be able to better understand the composition of the aircraft empty mass, FIGURE 8 shows the mass groups

of structure, energy, powertrain, and other systems group of the multirotor and their mass percentage in the total mass. The respective sum corresponds to the empty mass fraction in FIGURE 7.

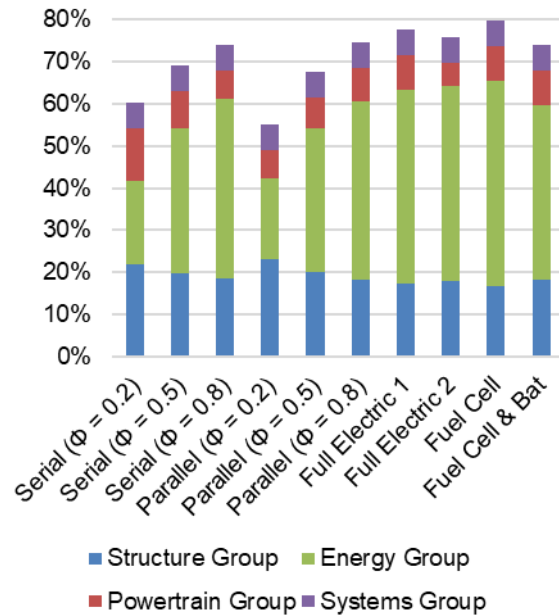


FIGURE 8. Mass fractions of the different groups

To determine the group masses, the masses of the individual components were calculated according to the models described in section 3.2. The assignment of the components to the groups was carried out as follows

- Structure Group: Fuselage, Landing Gear, Rotors; (the multirotor does not have wings or empennages)
- Powertrain Group: Electrical machines, gearboxes, power management, gas turbine
- Other Systems Group: Flight controls, avionics, furnishings, anti-icing
- Energy Group: Battery, fuel, fuel cell incl. thermal management, hydrogen

FIGURE 8 shows clearly, the largest mass fraction variation is in the energy group. The weight fractions of the other groups, on the other hand, vary only slightly. The fraction increases with the higher power ratio, i.e. the more energy is provided from the battery. The full electric systems therefore have the highest mass fractions in the energy group as well as the fuel cell systems.

It is known and documented across the literature that the battery mass can make up a very large proportion of the aircraft empty mass due to its low specific energy. To confirm this, FIGURE 9 shows the mass fractions of the battery and the fuel cell system. For the sake of clarity, the mass fractions of kerosene and hydrogen are very low compared to the battery and fuel cell and were neglected. As can be seen, the increasing empty mass and thus the total mass can be assigned to the impact of the battery mass or the fuel cell system.

If you want to achieve a lower aircraft weight MTOW or a higher payload ratio, the design driver is the battery mass (or respectively the fuel cell system).

To reduce this, you have to improve the battery technology, use an alternative hybrid-electric architecture or eventually a fuel cell system together with a battery. An investigation,

which was carried out by the author for a full electric and a serial hybrid-electric architecture, confirms the finding regarding the mass reduction with increasing battery technology level [15].

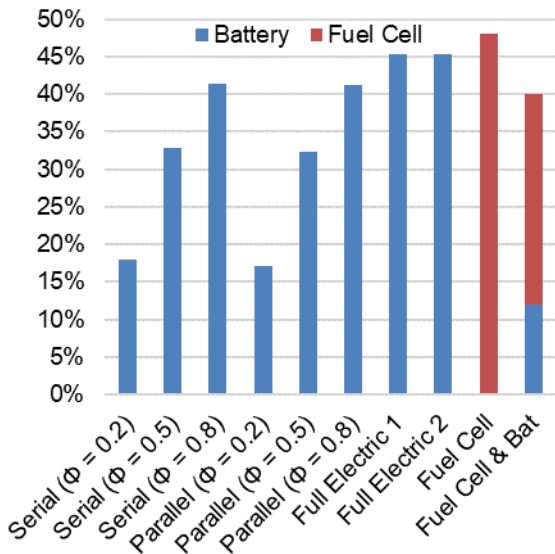


FIGURE 9. Battery and fuel cell mass fractions

#### 4.2.2. Required Power and Energy Efficiency

The different multirotor configurations were analyzed with regard to their power and energy requirements as well as their energy efficiency. For the sake of simplicity, only a few selected powertrain architectures are shown in the figures below. However, the results can be transferred to the other variants. Based on the initial flight mass (MTOM) and the design reference mission the required power can be calculated for each flight segment. The resulting net power over the flight time is shown in FIGURE 10. The higher the MTOM, the higher the net power. This means that the full electric with battery or the fuel cell system architecture have the highest net power.

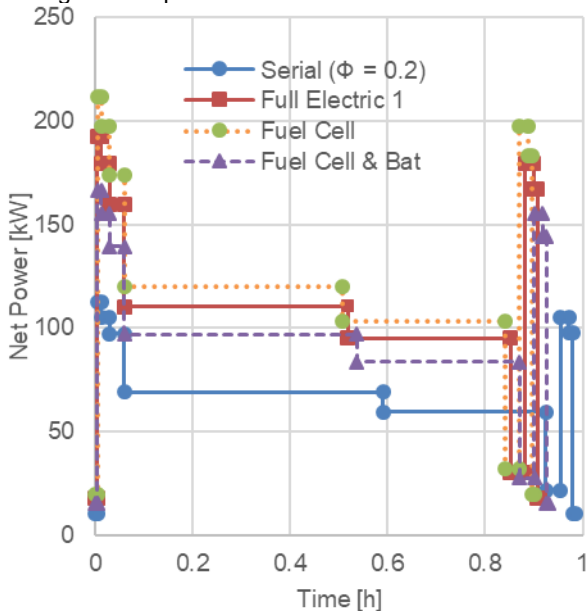


FIGURE 10. Aerodynamically required power (net power)

In order to calculate the required gross power from the energy sources, one must determine the total powertrain

efficiency with the efficiency of the various powertrain components (see TAB 4). In the case of hybrid-electric architectures, the supplied power ratio  $\Phi$  was also used. In the case of the "Fuel Cell & Bat" architecture, the efficiency was determined for each flight phase, as the ratio of power to total power (of both energy sources) and thus the efficiency changes. The required gross power, which was determined on the basis of net power and overall powertrain efficiency, is shown in FIGURE 11. The higher the efficiency, the lower the gross power. The full electric architecture therefore has the lowest gross power, although this is one of the heaviest architectures. The fuel cell system architectures require much gross power compared to the other architectures.

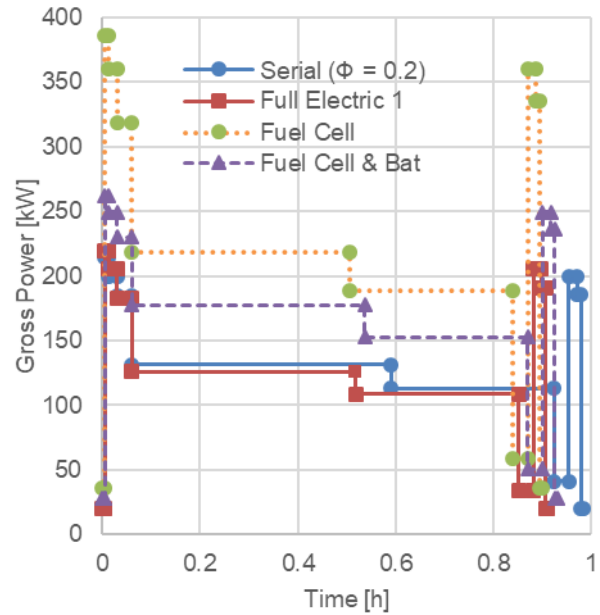


FIGURE 11. Required gross power

To calculate the consumed energy, the duration of each flight phase had to be calculated. This duration depends on the weight-dependent cruise speeds (see equations (11), (12)) and other specifications from TAB 3 and the mission profile (FIGURE 4). With the gross power and duration, the energy requirement of each flight phase and thus the total energy consumption for the entire mission could be determined. With the help of the number of passengers and kilometers traveled, the energy efficiency in the metric [Wh / PAX \* km] was calculated. This energy efficiency is shown in FIGURE 12 for the different architectures. Accordingly, the full electric architectures are the most efficient, while the architectures with fuel cell systems are the most inefficient.

If you want to design an overall energy-efficient system, the proportion of the battery should be selected to be relatively high, i.e. either a hybrid-electric architecture with a high supplied power ratio  $\Phi$  or full electric. There is still a need for research into how the architectures with fuel cell systems can be designed much more efficiently and how the technology should improve accordingly.

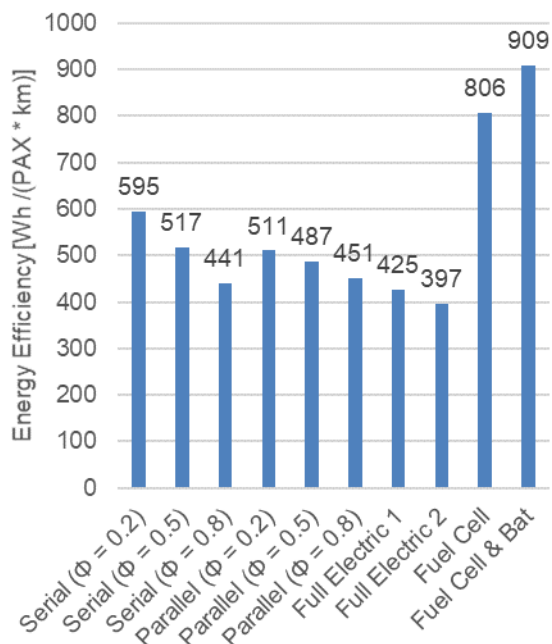


FIGURE 12. Energy efficiency

#### 4.2.3. Charging Power

In addition to the energy consumption, charging or refueling also plays an important role in assessing the feasibility of the multirotor configurations. In the following, the power of the battery charging station is determined for a given charging time. The charging time is important for the later operating concept of the multirotor at vertiports and the entire fleet. Refueling with kerosene or hydrogen is not considered in this work.

Based on the determined battery mass for each design, as well as the specific power of 250 Wh/kg and the usable energy factor of 80%, the battery energy amount is calculated. It is assumed that the calculated, usable battery energy also represents the maximum available battery capacity. In the case of batteries, the discharge current is often given via the C-rate. The C-rate relates the discharge current to the maximum capacity of the battery. Assuming a C-rate of 3, which means a charging time of 20 min for the determined maximum battery capacity, the power for the battery charging station can be calculated. The calculated charging capacities for the different variants are shown in FIGURE 13.

According to the current state of the art, there are already existing ultra-fast charging stations for electric-powered, ground-based vehicles between 150 kW and 350 kW. Assuming that corresponding charging stations can also be used in the area of UAM vehicles, the basic feasibility of recharging can be determined for nearly all architectures except the full-electric powertrains. The higher the fraction of electrical energy, the higher the required charging power of the station.

However, if you want to achieve faster charging times, this also results in a higher C-rate for the battery. According to the state of the art, batteries can be charged or discharged at a higher C-rate. However, the thermal load also increases, which can lead to thermal runaway with the dangers described in section 2.3 as well as a reduced service life. In addition, if the C-rate doubled, the charging

power would also double, i.e. the current availability of such charging stations is not yet guaranteed.

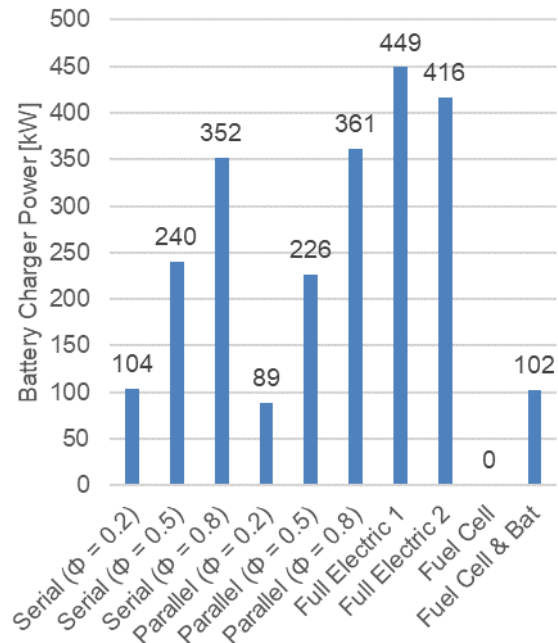


FIGURE 13. Battery charger power for C-Rate of 3/h and charging time of 20 min

#### 4.3. Final Evaluation

On the basis of the defined study, different powertrain systems were examined in more detail based on a simple, generic and sizeable multirotor configuration. The aim of the study was to get deeper knowledge and, if possible, to identify suitable and feasible concepts for a propulsion architecture. The results show that all configurations are feasible. The mission requirements were met, the maximum take-off mass was clearly under the allowable mass and the possibility of recharging was successfully investigated.

It could be mathematically proven that the battery and respectively the fuel cell system are important design drivers of the aircraft mass. If you want to achieve a lower overall mass or a higher ratio of payload to total mass, an optimal architecture must be found here. It was also found that the overall efficiency of the powertrain system and its operation (e.g. via power control parameters) is the influencing factor for the energy efficiency of the vehicle. Here, the "simple" full electric powertrain systems have a clear advantage over the hybrid-electric and systems with fuel cells, which have to be examined in more detail. Fuel cell systems should be more suitable for longer distances. In the future it is therefore necessary to investigate the dependency of sensible powertrain architecture from the TLARs (e.g. design reference mission), especially with respect to fuel cells. For further research, a full electric architecture as well as an architecture with fuel cell and batterie will be more investigated.

The design methodology developed and used is based on relatively simple models and assumptions. The results should in view of specific values therefore be used with a certain amount of caution. Nevertheless, the qualitative and quantitative results can be confirmed with the help of the findings from the literature as well as in the order of magnitude (e.g. masses, power).

## 5. SUMMARY AND OUTLOOK

At the German Aerospace Center (DLR) research is being carried out in the field of Urban Air Mobility (UAM). In the internal project HorizonUAM one of the goals is the development of a system concept for an air taxi. To this end, the Safety-critical Systems and Systems Engineering department at the DLR Institute of Flight Systems conducts research in the field of safe and certifiable onboard systems.

The aim of this article is to give an overview of the previous results and findings. For this purpose, the system and safety-related challenges in the design of the onboard systems were described in chapter 2. A special focus was set on electric powertrain systems. In chapter 3 a conceptual design methodology was described, which makes it possible to examine full, turbo- and hybrid-electric powertrain systems in the context of the multirotor design. This methodology was used in chapter 4 to investigate the influence of different powertrain architectures on the multirotor design.

It was found that the battery and the fuel cell system have an important impact on the aircraft mass. Improved battery technology results in a reduction in mass [15], but this technology must also be available in near future and be inexpensively. Alternatively, hybrid electrical architectures can be used as bridge technology or powertrains with fuel cell systems. However, these in turn have the disadvantage of poorer energy efficiency compared to full electric powertrains. In principle, however, it can be stated that under the defined boundaries and design requirements, the investigated systems can be implemented in principle.

The design methodology described above will be further developed in future work. The application of this methodology will be mainly in the area of varying the requirements, mission and technology parameters in order to identify further design drivers and limitations. Furthermore, the methodology has already been integrated into a higher-level system of systems simulation in order to show the influence of the onboard systems on the design and operation of an UAM system [15].

For further research, a full electric architecture as well as an architecture with fuel cells and batteries will be investigated. Research will be carried out with regard to the safety-critical design as well as thermal management of these powertrain systems, safety and reliability analyzes, certification aspects and the overall modeling of the onboard systems.

## 6. ACKNOWLEDGMENTS

The research activities are funded with internal project funds as part of the DLR project HorizonUAM.

## 7. REFERENCES

- [1] B. Schuchardt. "HorizonUAM-Urban Air Mobility Research at the DLR German Aerospace Center". In: e-Flight Forum China 2020.
- [2] O. Bertram et al. "Stand der Technik und Forschung zu Bordsystemen von Lufttaxi". DLR internal report, DLR-IB-FT-BS-2021-93. 2021
- [3] M. Hirschberg. "The Electric VTOL Revolution", 2019.
- [4] W. Johnson et. al. "Concept Vehicles for VTOL Air Taxi Operations", 2018.
- [5] B. A. Hamilton. "UAM Market Study - Technical Out Brief", 2018.
- [6] B. Brelje et al. "Electric, Hybrid, and Turboelectric Fixed-wing Aircraft: A Review of Concepts, Models, and Design Approaches". *Progress in Aerospace Sciences*. 2019, vol 104, p. 1–19.
- [7] R. de Vries et al. "Preliminary Sizing Method for Hybrid-electric Distributed-propulsion Aircraft". *Journal of Aircraft*, 2019, 56. Jg., Nr. 6, S. 2172-2188.
- [8] P. Kurzweil. "Brennstoffzellentechnik", Springer-Verlag, Fachmedien Wiesbaden, 2013.
- [9] EASA. "Special Condition for VTOL Aircraft". 2019.
- [10] EASA. "Proposed Means of Compliance with the Special Condition VTOL". 2020.
- [11] G. J. Leishman. "Principles of Helicopter Aerodynamics". Cambridge University Press, 2006.
- [12] F. Barra et al. "A Methodology for Multirotor Aircraft Power Budget Analysis". *Aircraft Engineering and Aerospace Technology*. 2020.
- [13] J. M. Vegh et al. "Current Capabilities and Challenges of NDARC and SUAVE for eVTOL Aircraft Design and Analysis". In: 2019 AIAA/IEEE Electric Aircraft Technologies Symposium (EATS). IEEE, 2019. S. 1-19.
- [14] A. R. Kadhiresan et al. "Conceptual Design and Mission Analysis for eVTOL Urban Air Mobility Flight Vehicle Configurations". In: AIAA Aviation 2019 Forum. 2019. S. 2873.
- [15] P. Prakasha et al. "System of Systems Simulation driven Urban Air Mobility Vehicle Design and Fleet Assessment". AIAA Aviation Forum, AIAA-2021-3200, 2021.

## APPENDIX

Pow ertrain Architecture / Configuration Name	Serial ( $\Phi = 0.2$ )	Serial ( $\Phi = 0.5$ )	Serial ( $\Phi = 0.8$ )	Parallel ( $\Phi = 0.2$ )	Parallel ( $\Phi = 0.5$ )	Parallel ( $\Phi = 0.8$ )	Full Electric 1	Full Electric 2	Fuel Cell	Fuel Cell & Bat
<i>Multirotor Characteristics</i>										
No. of Rotors N	4	4	4	4	4	4	4	4	4	4
Disc Loading [N/m <sup>2</sup> ]	140	140	140	140	140	140	140	140	140	140
Rotor Radius [m]	2.32	2.60	2.81	2.19	2.55	2.85	3.03	2.92	3.18	2.82
Total Disc Area [m <sup>2</sup> ]	67.47	85.15	99.35	60.47	81.53	102.21	115.53	107.26	126.87	99.81
Single Disc Area [m <sup>2</sup> ]	16.87	21.29	24.84	15.12	20.38	25.55	28.88	26.82	31.72	24.95
Blade Tip Speed [Mach]	0.45	0.45	0.45	0.45	0.45	0.45	0.45	0.45	0.45	0.45
Equivalent Flat Plate Area [m <sup>2</sup> ]	3.0	3.0	3.0	3.0	3.0	3.0	3.0	3.0	3.0	3.0
<i>Masses</i>										
MTOM [kg]	963.2	1215.6	1418.3	863.3	1163.9	1459.2	1649.4	1531.3	1811.2	1424.9
Payload [kg]	360.0	360.0	360.0	360.0	360.0	360.0	360.0	360.0	360.0	360.0
Empty Mass [kg]	603.2	855.6	1058.3	503.3	803.9	1099.2	1289.4	1171.3	1451.3	1065.0
Structural Group [kg]	198.5	229.9	253.6	185.4	223.6	258.3	279.5	266.4	297.1	254.4
Wings, Empennage [kg]	0.0	0.0	0.0	0.0	0.0	0.0	0.0	0.0	0.0	0.0
Fuselage [kg]	117.3	131.5	141.8	111.2	128.7	143.8	152.7	147.3	159.9	142.2
Landing Gear [kg]	43.7	51.1	56.6	40.6	49.6	57.7	62.7	59.6	66.7	56.8
Rotor [kg]	37.5	47.3	55.2	33.6	45.3	56.8	64.2	59.6	70.5	55.4
Pow ertrain Group [kg]	111.8	103.6	92.8	53.3	82.6	113.0	133.2	85.4	146.3	115.1
Gasturbine [kg]	20.5	12.7	4.8	17.1	11.8	5.0	0.0	0.0	0.0	0.0
Gearbox [kg]	16.9	10.4	4.0	20.6	27.7	34.8	39.3	0.0	43.2	34.0
Pow er Mgmt. [kg]	24.2	30.5	35.6	7.0	19.4	32.9	42.2	38.4	46.4	36.5
Electr. Machines [kg]	50.3	12.7	48.5	8.6	23.7	40.3	51.7	47.0	56.8	44.7
Energy Group [kg]	181.1	37.3	589.1	155.3	381.0	604.3	748.5	694.0	875.9	572.7
Battery [kg]	172.8	404.3	587.4	148.1	376.5	602.5	748.5	694.0	0.0	170.8
Fuel [kg]	8.3	4.8	1.8	7.1	4.5	1.8	0.0	0.0	0.0	0.0
Fuel Cell [kg]	0.0	0.0	0.0	0.0	0.0	0.0	0.0	0.0	869.0	399.0
Hydrogen [kg]	0.0	0.0	0.0	0.0	0.0	0.0	0.0	0.0	6.9	2.9
Systems Group [kg]	111.8	0.0	122.7	109.4	116.6	123.7	128.2	125.4	132.1	122.8
<i>Mass Fractions</i>										
Payload [%]	40%	31%	26%	45%	32%	25%	22%	24%	20%	26%
Empty Mass [%]	60%	69%	74%	55%	68%	75%	78%	76%	80%	74%
Structure Group [%]	22%	20%	18%	23%	20%	18%	17%	18%	17%	18%
Pow ertrain Group [%]	12%	9%	7%	7%	7%	8%	8%	6%	8%	8%
Energy Group [%]	20%	35%	43%	19%	34%	43%	46%	46%	49%	41%
Systems Group [%]	6%	6%	6%	6%	6%	6%	6%	6%	6%	6%
Battery Mass Fraction [%]	17.9%	33.3%	41.4%	17.2%	32.3%	41.3%	45.4%	45.3%	0%	12.0%
Fuel Mass Fraction [%]	0.9%	0.4%	0.1%	0.8%	0.4%	0.1%	0%	0%	0%	0.0%
Fuel Cell Mass Fraction [%]	0%	0%	0%	0%	0%	0%	0%	0%	48.0%	28.0%
Hydrogen Mass Fraction [%]	0%	0%	0%	0%	0%	0%	0%	0%	0.4%	0.2%
<i>Power Characteristics</i>										
Supplied Pow er Ratio $\Phi$	0.2	0.5	0.8	0.2	0.5	0.8	1.0	1.0	1.0	1.0
Battery Spec. Energy [Wh/kg]	250.0	250.0	250.0	250.0	250.0	250.0	250.0	250.0	250.0	250.0
Pow ertrain Efficiency [%]	52.5%	66.4%	80.2%	56.7%	68.3%	79.9%	87.6%	89.4%	54.7%	63.4%
Energy Eff. [Wh/ Pax*km]	595.5	516.7	441.4	510.8	486.6	451.2	425.5	397.1	806.4	909.3
Hover Pow er [kW]	105.0	132.5	154.5	94.1	126.8	159.0	179.7	166.9	197.4	155.3
Cruise Pow er [kW]	69.2	84.6	96.7	63.0	81.4	99.1	110.3	103.4	119.8	97.1
Total Consumed Energy [kWh]	124.6	116.8	108.3	106.7	110.0	111.0	110.9	102.8	190.3	156.7
Useable Battery Energy [kWh]	34.6	79.9	117.5	29.6	75.3	120.5	149.7	138.8	0.0	34.2
C-Rate Charging [1/h]	3	3	3	3	3	3	3	3	3	3
Battery Charging Time [min]	20	20	20	20	20	20	20	20	0	20
Battery Charger Pow er [kW]	103.7	239.7	352.4	88.9	225.9	361.5	449.1	416.4	0.0	102.5
Best Range Speed [km/h]	86.7	91.9	95.5	84.3	90.9	96.2	99.2	97.3	101.5	95.6
Best Endurance Speed [km/h]	65.9	69.8	72.6	64.1	69.1	73.1	75.3	74.0	77.1	72.6
Flight Duration [min]	59.1	57.1	55.9	60.0	57.5	55.7	54.7	55.3	54.0	55.9

TAB 5. Multirotor design parameters and results